ELSEVIER

Chemical Engineering Journal 139 (2008) 532–539

Chemical Engineering Journal

www.elsevier.com/locate/cej

Catalytic properties of carbon nano-filaments produced by iron-catalysed reforming of ethanol

Sepideh Jankhah, Nicolas Abatzoglou *, François Gitzhofer, Jasmin Blanchard, Hicham Oudghiri-Hassani

Université de Sherbrooke, Department of Chemical Engineering, 2500 Boul. Université, Sherbrooke, Québec, Canada J1K 2R1

Received 30 May 2007; received in revised form 9 August 2007; accepted 24 August 2007

Abstract

Various applications for carbon nano-filaments (CNF), such as polymer additives, gas storage materials and catalyst supports have recently been reported. The present work focuses on the catalytic properties of carbon nano-filaments, as produced through the catalytic dry reforming of ethanol, using low-carbon steel as the catalyst. It has been quantitatively demonstrated that these carbon nano-filaments have high catalytic activity in respect of the ethanol dry reforming and cracking reactions. Iron carbide particles, encapsulated in the CNF, are shown to be the active agents possessing the observed catalytic properties. The exact reaction mechanism of this process is still unknown.

Keywords: Dry reforming; Ethanol; Catalysis; Carbon nano-filaments; Hydrogen; Carbon steel; CO_2 sequestration

1. Introduction

For the first 80 years of the last century, the occurrence of carbon nano-filaments (CNF) in certain chemical processes was considered a nuisance. However, recently several researchers have explored the use of CNF in several applications, such as additives in polymers [1,2], as gas storage media [3] and as catalyst support material. In particular, Sui et al. [4] have studied their properties as an effective support for catalysts used in ethanol partial oxidation reactions. Other research groups have also used CNF products; as catalysts supports [5,6], or as an actual catalyst for the oxidative hydrogenation (ODH) of ethyl-benzene, to produce styrene [7].

In the work reported by Sui et al. [4], in order to remove the metal-based inclusions, the used CNF was repeatedly washed in 2 mol/l HCl over a 7-day period, followed by thorough washing of the filtered CNF with large amounts of de-ionised water, until the filtrate was neutral (at a pH value close to 7), then dried at 120 °C overnight. Baker et al. [6], who also used the CNF as catalyst support, have previously removed the occluded metal-based particles through dissolution in 1 M HCl and further thorough washing in de-ionised water, before an overnight air drying treatment at 110 °C. In the present work, the "as synthesised" CNF, without any special pre-treatment, have been tested for their catalytic activity in ethanol dry reforming/ethanol cracking reactions.

Recent published work by the authors has shown that the catalytic dry reforming of ethanol can (a) produce a H_2-rich synthesis gas, and (b) sequester gaseous CO_2 under the form of solid CNF, using iron alloy catalysts [8,9]. It has also been shown that a two-step, thermal-oxidative activation pre-treatment of the carbon steel is necessary.

The present work examines the catalytic properties of CNF, produced through ethanol dry reforming and ethanol cracking reactions. For this purpose, the conversion of ethanol and CO_2, as well as the compositions and volumes of gases, produced in both the presence and the absence of CNF, are compared to those obtained in tests using carbon steel as the catalyst. The CNF produced were analysed by scanning electron microscopy (SEM) and transmission electron microscope (TEM) to simultaneously explore their structures, size distribution and homogeneity. SEM analyses have confirmed the presence of iron-based particles encapsulated in the produced CNF. Elemental and X-ray diffraction analyses of the CNF product have determined that the sub-particles, found inside their structures, are mainly composed of iron carbides. The latter part of this work reports the results

* Corresponding author. Tel.: +1 819 821 7904.
E-mail address: Nicolas.Abatzoglou@USherbrooke.ca (N. Abatzoglou).

1385-8947/$ – see front matter © 2007 Elsevier B.V. All rights reserved.
doi:10.1016/j.cej.2007.08.031

of a series of experiments that have shown that the activity of the CNF is related to the presence of these iron carbide particles. The turnover frequency (TOF) values, defined as the rate of products generation over the quantity of iron present in the catalyst, were calculated in order to compare the catalytic activity of the CNF with that of the carbon steel. The iron content in the CNF was obtained by standard atomic absorption (AA) analyses.

Since the exact number of the active sites is not known, due to a lack of knowledge regarding the catalytic mechanism, the quantity of Fe was chosen as being representative of the active sites. The assumption is that all iron compounds, as used in all of the tests, have the same density of active sites (number of active sites per unit mass of Fe). As mentioned by Boudart [10], TOF is a chemical reaction rate, dependant on the temperature, pressure and concentration values. The advantage of calculating the TOF is that even if a TOF value is only approximate, because of the approximations made in counting the catalytically active sites, it is nevertheless useful for assessing the potential of new catalytic materials, in relation to those catalysts still in current use.

2. Methodology

2.1. Experimental setup and analyses

A quartz, bench-scale, fixed-bed reactor (BSFBR), with a diameter of 4.6 cm and a length of 122 cm, was used. The reactor conditions were set at 550 °C and 1 atm. Liquid ethanol (98–99.9%, v/v) was pumped from a reservoir and then vaporised before entering the reactor. CO_2 or Ar gases were added to the ethanol vapour upstream of the reactor. All gases were supplied by Praxair, their purity values being 99.99% for both CO_2 and Ar (Fig. 1).

The carbon steel catalyst was AISI 1010 and contained a maximum of 0.13% C, 0.3–0.6% Mn, a maximum of 0.04% P and a maximum of 0.05% S. The sheet thickness was 0.13 mm (±10%) and the UPC number was 13320(16AS). All herein reported material content percentages are in w/w. The catalyst consisted of two strips of carbon steel, 1.8 cm wide, 58 cm long and weighing 20.5 g. The catalyst was "fixed" on the quartz tube which also contained the central thermocouple located at the reactor center. The exit gas was dried, using a cold trap and a molecular sieve column, and then analysed, using a GC Model CP3800 from Varian Inc. (HayeSep Q CP81073, HayeSep Q 81069, and HayeSep T CP81072 columns and Molsieve 13× CP81071 and Molsieve 5A CP81025, with column temperatures maintained at 50 °C).

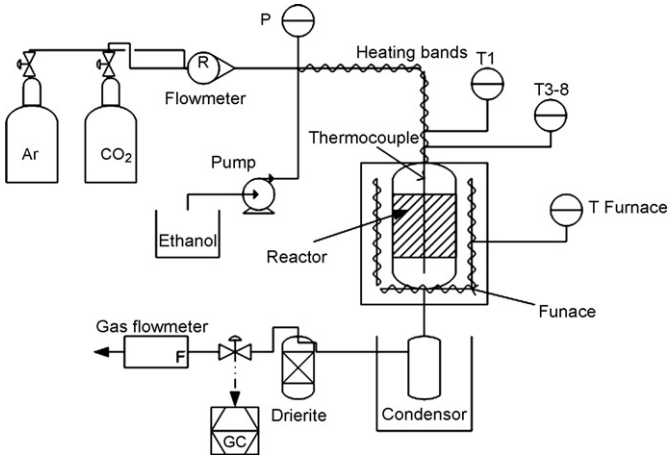

Fig. 1. Experimental set-up.

A high resolution scanning electron microscope (SEM) Hitachi S-4700 was used for both high quality imaging and for the elemental analyses of the CNF. XRD analyses were obtained by a Panalytical X'pert Pro diffractometer, using Cu Kα radiation at room temperature, and with instrumental settings at 45 kV and 40 mA; the XRD analyses being used to detect the crystalline phases present in the CNF.

AA analyses of the CNF were performed by flame spectroscopy in order to determine the quantity of iron present in the produced CNF. For this purpose, a Varian SpectrAA-50/55 spectrometer was used, being equipped with a 5 mA Fe lamp with working wavelength set at 372.0 nm, along with acetylene fuel flame and air support. The analysis of each CNF sample was repeated three times, and the average relative standard deviation (R.S.D.) percentage was of 0.6%.

2.2. Experimental procedure

The experimental work performed consisted of:

- *Step 1*. Dry reforming of ethanol, using low-carbon steel as the catalyst; this step produced the tested CNF;
- *Step 2*. Ethanol cracking and dry reforming tests, using the produced in step 1 CNF as catalyst.

Dry reforming reactions of step 1 were conducted in the fixed-bed, isothermal reactor, at 550 °C over a 2 h period using the above-described pre-treated strips of carbon steel as catalyst. The molar ratio of the input ethanol/CO_2 reactants was 1, and when catalysts were used, the overall gas hourly space velocity (GHSV) was of 2 300 ml/(h g) and 1.15 $m^3/(h\,m^2)$, based on the geometrically calculated surface area of the catalyst (the strips of carbon steel are non-porous and consequently the internal surface is negligible). In order to keep equivalent reaction conditions in the tests without catalysts, the chosen gas flow rates remained the same.

The catalyst employed in step 1 consisted of a sheet of low-carbon (0.1%) steel, having been thermally pre-treated at 800 °C and then, partially oxidised at 550 °C [8]. Carbon nanostructures were formed on the carbon steel catalyst surface during the reforming reaction, being denoted as "first generation CNF", and were shown to have diameters ranging between 5 and 200 nm (Fig. 2). They are recovered by mechanical means and subsequently "analysed", using SEM, TEM, field emission gun scanning electron microscope (FEGSEM) and XRD methods.

The following experiments of step 2 were designed to study the catalytic properties of the CNF products:

1. Liquid ethanol, at a flow rate of 0.33 ml/min, Ar at a flow rate of 140 ml_{STP}/min (STP: standard temperature and pressure) glass wool as the support.

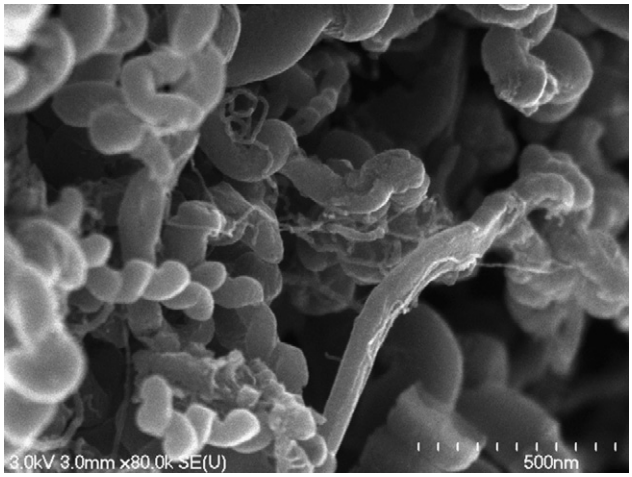

Fig. 2. SEM analysis of first-generation CNF.

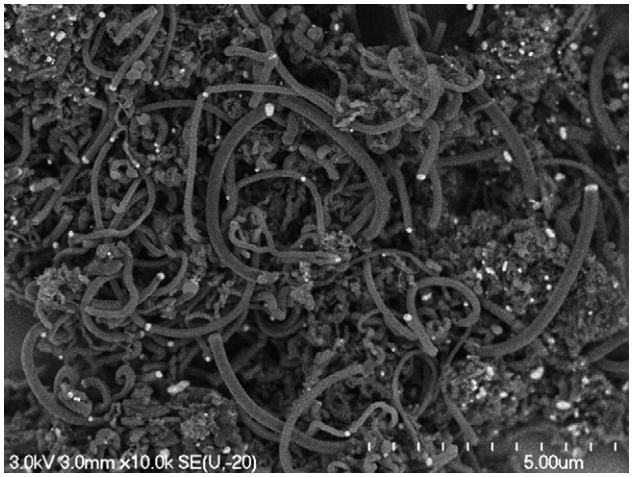

Fig. 3. SEM of preliminary CNF.

2. Liquid ethanol at a flow rate of 0.33 ml/min, CO_2 at a flow rate of 140 ml_{STP}/min, glass wool as the support.
3. Liquid ethanol at a flow rate of 0.33 ml/min, Ar at a flow rate of 140 ml_{STP}/min, 4 g CNF as the catalyst, glass wool as the support.
4. Liquid ethanol at a flow rate of 0.33 ml/min, CO_2 at a flow rate of 140 ml_{STP}/min, 4 g CNF as the catalyst, glass wool as the support.

The CNF used as the catalyst was "fixed" at the reactor center, using an inert dispersion matrix of glass wool (3 g), supported on the tubular quartz cover of the central thermocouple. Tests, without CNF being present, were performed to set a "reference point" for the ethanol thermal cracking and thermal dry reforming reactions. Tests with ethanol (EtOH) and Ar (i.e., the absence of CO_2) were planned in order to study the catalytic properties of the CNF, with respect to the ethanol cracking reaction. The temperature was set at 550 °C for both the cracking and dry reforming tests, in order to maximise carbon formation (i.e., conditions thermodynamically favouring carbon formation). The molar ratio of the input EtOH/Ar was set at 1. Ar was added in the case of thermal cracking in order to maintain the same overall GHSV, and consequently, to have the same ethanol concentration present in the gaseous reactants at the entrance of the reactor, as in the tests performed with CO_2. Tests with EtOH and CO_2 were planned to study the catalytic properties of the CNF in the dry reforming reaction. The operating parameters for the reaction of ethanol and CO_2 are the same as for the ethanol dry reforming case, using the carbon steel catalyst.

SEM analyses on the CNF product demonstrated the presence of particles encapsulated in their tubular structures (Fig. 3). Elemental analyses of the CNF (Fig. 4) showed that these particles were composed of iron, oxygen and carbon. In addition, the XRD analyses (see Fig. 5) showed that these particles were mainly composed of iron carbides. Following the initial reaction tests, an additional series of experiments was set-up in order to study the effect of the particles, encapsulated in the CNF, on the catalytic activity of the latter. Although it was found by the XRD analyses that "encapsulated" particles in the CNF

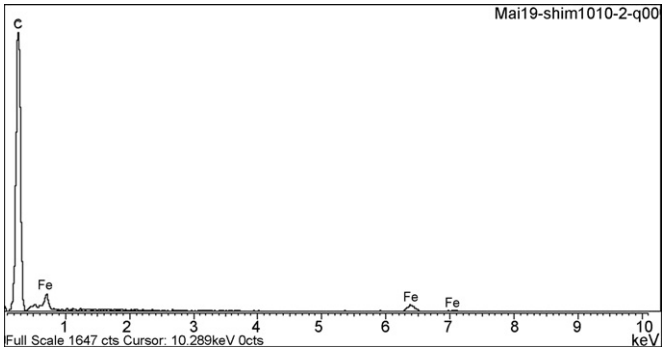

Fig. 4. Elemental analysis of CNF.

are mainly composed of iron carbide(s), their exact role in the reforming reactions remains still unknown. Thus, the mass of Fe was chosen to be representative of the amount of catalytically active sites for the reforming reactions taking place. The actual amount of iron present in the CNF was obtained by AA analysis.

For the purpose of studying the effect of encapsulated particles on the catalytic properties of CNF, some 25 g of a "first generation" CNF was produced, via the reaction of ethanol dry

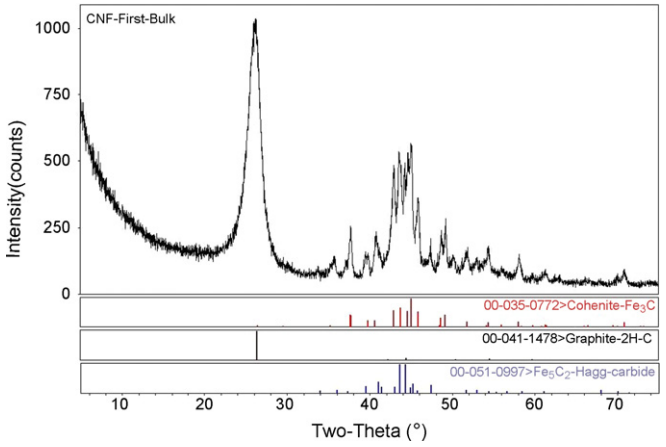

Fig. 5. XRD analysis of the bulk of first-generation CNF.

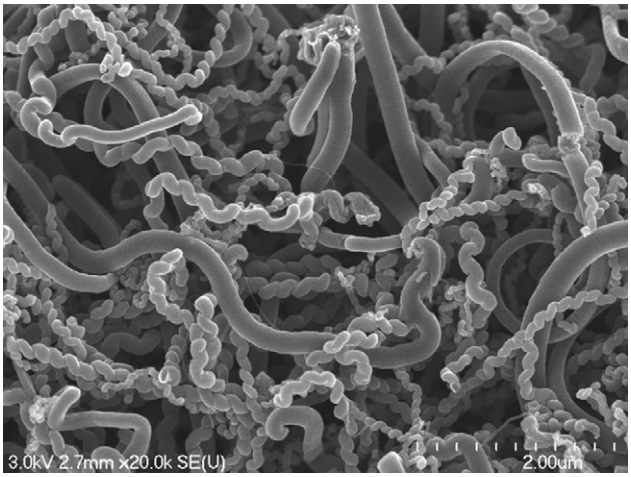

Fig. 6. SEM analysis of second-generation CNF.

reforming, using carbon steel as the catalyst [8]. An additional series of experiments was designed as follows:

1. A 2 h ethanol dry reforming experiment was performed, under operating conditions as described above, using 4 g of "first generation" CNF as the catalyst. The GHSV in the experiment, using the "first generation" CNF as the catalyst, was 121 000 ml/(h g), based on the quantity of Fe measured in the CNF, by AA analysis. The total weight of CNF recovered, at the end of reaction, was 7.95 g. The carbon produced, named as the "second generation" CNF, was analysed by SEM, and was also under the form of CNF (Fig. 6).
2. This "second generation" CNF was thoroughly homogenised and 4 g of the resulting material were used as the catalyst for another reforming experiment; at the end of the reforming experiment 7.7 g of a third generation carbon product was obtained. The GHSV in this experiment was 348 000 ml/(h g), based on the quantity of Fe present in the second generation CNF. This third generation material also proved to be in the form of CNF (Fig. 7).

Fig. 7. SEM analysis of third-generation CNF.

3. The same procedure was repeated to produce a fourth generation CNF product, through the reforming reaction of ethanol, from the third generation CNF. The GHSV was 790 000 ml/(h g), based on the quantity of Fe present in the third generation CNF.

The experiment operating conditions, the produced gas composition and the mass of carbon nano-filaments produced, are shown in Table 2. By mixing and dividing the homogenised CNF into two equal mass samples at each step, we intrinsically made the hypothesis that the quantities of particles encapsulated in the CNF are also equally divided by 2. The precise quantities of Fe found in the "different generations" of the CNF product, as obtained by AA analyses, are shown in Table 2. It can be seen that this hypothesis cannot be rejected statistically. All tests were performed in the previously described, bench-scale isothermal, fixed-bed quartz reactor. The composition of the gas produced was analysed by means of the "on-line" gas chromatograph.

3. Results

3.1. CNF as the catalyst of ethanol dry reforming and ethanol cracking

The results of the series of ethanol dry reforming and ethanol cracking experiments described above are summarised in Tables 1 and 2.

The results of the reforming experiments, using carbon steel and CNF as the catalyst, can be compared by reference to Table 2. As set out, the first generation of CNF product shows 100% conversion of the input ethanol. The volume of H_2 and CO gases produced is also comparable to the volumes of H_2 and CO produced by the "dry reforming" of ethanol with carbon steel. It is seen that the quantity of Fe present in the 1st generation CNF, used as the catalyst for the production of the 2nd generation CNF, is 1/53 times the quantity of iron present in the carbon steel used as the catalyst. However, its TOF is 46 times the TOF of the 1st generation CNF experiment. This observation indicates that the 1st generation CNF is slightly less active than the carbon steel catalyst, but this difference could be due to the systematic experimental error.

The results of the experiments performed in the absence of and the presence of CNF, can also be compared in Table 2. In the ethanol dry reforming experiments, using first generation CNF as the catalyst, the ethanol conversion was 99%, while without the CNF catalyst, ethanol conversion was reduced to only 43%. A 100% increase in the CNF mass was also observed in the presence of the CNF, while no carbon was deposited on the surfaces of the glass wool used in the experiment performed without CNF. The volume of the H_2 produced, through the dry reforming of ethanol in the presence of CNF, was about 20 times the volume of H_2 obtained under the same operating conditions, but without the CNF.

In the case of the experiment with EtOH/Ar, the volume of H_2, produced through the cracking of ethanol in presence of CNF, was some 10 times the volume of hydrogen obtained under the same operating conditions without CNF. Ethanol conversion in

Table 1
Results of the dry reforming with different generations of CNF

Generation of CNF	Exit flow, H_2 (ml/min)	Exit flow, CO_2 (ml/min)	Exit flow, CH_4 (ml/min)	Exit flow, CO (ml/min)	Conversion%, EtOH	Conversion%, CO_2
1st	323	95	18	181	99.8	32.1
2nd	278	120	21	155	99.1	14.2
3rd	260	141	19	138	92.0	0.0
4th	189	142	20	108	90.6	−1.0

presence of the first generation CNF was 96.8%, while the conversion was only 46.1% for the experiment of EtOH/Ar, without CNF. A 180% increase in the CNF mass was observed in the presence of CNF, while no carbon was deposited on the surface of the glass wool in the experiment without CNF.

The greater volumes of the H_2 and CO gases produced, as well as the higher conversion levels of ethanol, along with the deposition of carbon nano-filaments, observed in the experiments performed with CNF, proves, once again, that the CNF, formed through the dry reforming reaction of ethanol over the carbon steel catalyst, is an active catalyst for both the ethanol cracking and the dry reforming reactions.

The first generation, carbon nano-filaments were analysed before being used as catalysts. The Brunauer–Emmett–Teller (BET) (N_2) surface area values of the nano-filaments range from 125 to 155 m^2/g, depending on the particular structural conformation adopted. TEM analysis (Fig. 8) demonstrates that these tubular carbon filaments have multilayer structures. The average diameter for the primary produced CNF was between 100 and 200 nm, while a few nano-filaments were also found in the diameter range of 5–50 nm (see Fig. 2).

In the SEM analyses of the first generation CNF, the existence of agglomerations of carbon that contain higher concentrations of catalyst particles than the carbon filaments (Fig. 9a) were observed. This can be explained by the fact that the first generation CNF also includes the layer of carbon, deposited directly on the surface of the carbon steel catalyst; this layer was removed by mechanical means and was added to the bulk of the CNF. The carbon that was in contact with the metal surface contains the highest amounts of catalyst particles. The XRD analyses (Figs. 4–10), as reported later in this article, validate this hypothesis.

Table 2
Successive reforming reactions

Test	1st generation CNF catalyst	2nd generation CNF catalyst	3rd generation CNF catalyst	4th generation CNF catalyst	Catalytic cracking reaction	Thermal reforming	Thermal cracking
EtOH (ml/min)	0.35	0.33	0.33	0.36	0.34	0.35	0.35
CO_2 (ml/min)	140	140	140	140	0	140	0
Weight of catalyst (g)	20.58	4.00	4.11	3.87	3.94	0	0
Duration (min)	120	120	120	120	120	78	75
Type of catalyst	Carbon steel	CNF (1st)	CNF (2nd)	CNF (3rd)	CNF (1st)	No catalyst	No catalyst
Support	Glass wool	Glass wool	Glass wool	Glass wool	Glass wool	Glass wool	Glass wool
Iron % in CNF produced	9.5	3.2	1.6	0.6	3.3	N/A	N/A
Iron % in CNF catalyst	100	9.5	3.2	1.6	9.5	0	0
Fe in catalyst (g)	20.58	0.38	0.13	0.06	0.36		
GHSV (ml/(h g))	2 301	120 955	348 155	789 367	124 774	N/A	N/A
Total produced carbon (g)	6.75	3.90	3.58	2.80	7.28	0	0
Rate of carbon production (g/min)	0.056	0.033	0.030	0.023	0.061	0	0
Mole C/Mole CO_2	0.820	0.474	0.434	0.340		0	0
Exit gas (ml/min)	633	619	583	495	584	190	45
EtOH conversion	99.8%	99.1%	92.0%	90.6%	96.8%	43.6%	46.1%
CO_2 conversion	32.1%	14.2%	−0.5%	−1.1%		−18.4%	
Exit liquid EtOH (ml)	0.08	0.34	3.17	3.99	1.32	18.17	16.94
Exit liquid water (ml)	3.52	2.49	3.05	4.37	2.73	2.48	3.58
H_2 (ml/min)	323	278	260	189	395	15	30
CO (ml/min)	181	155	138	108	73	4	6
CO_2 (ml/min)	95	120	141	142	16	166	0.1
CH_4 (ml/min)	18	21	19	20	21	6	8
TOF(H_2) (s^{-1})	0.00002	0.00099	0.00267	0.00424	0.00143		
TOF(CO) (s^{-1})	0.00017	0.00777	0.01984	0.03390	0.00369		
TOF(CO_2) (s^{-1})	0.00014	0.00944	0.03184	0.06994	0.00124		
TOF(CH_4) (s^{-1})	0.00001	0.00060	0.00153	0.00361	0.00061		
$T_{reaction}$ (°C)	550	550	550	550	550	550	550
C balance error	−0.03	−0.09	−0.04	0.04	0.15	0.14	0.30
H balance error	0.00	−0.06	0.00	0.12	−0.13	0.17	0.10
O balance error	0.03	−0.02	−0.11	−0.06	0.02	−0.12	−0.13

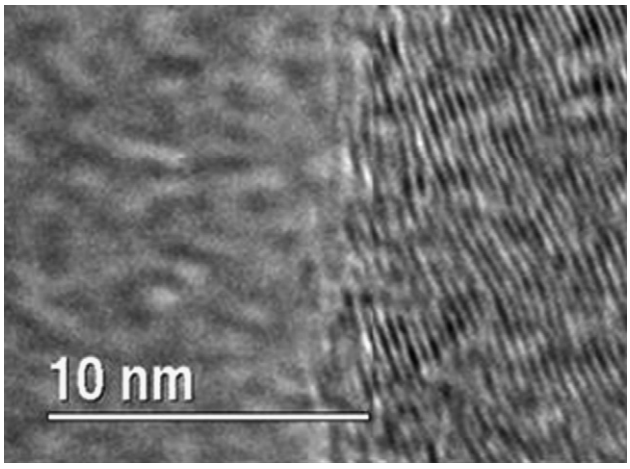

Fig. 8. TEM analysis of CNF.

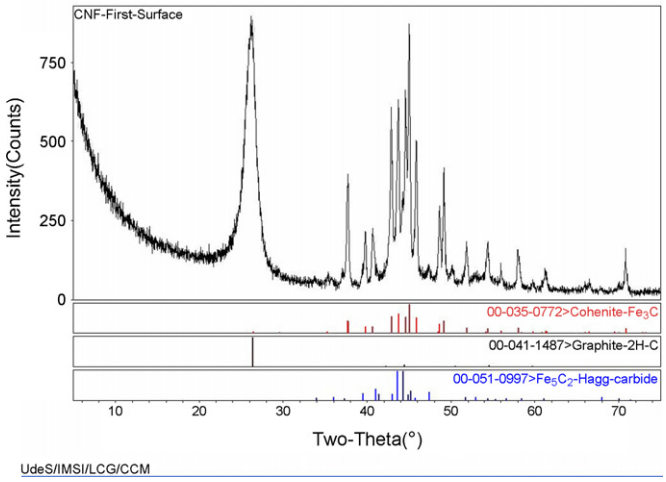

Fig. 10. XRD analysis of the thin layer of CNF deposited on the catalyst surface.

3.2. Catalytic properties of CNF: active iron carbide particles

The carbon deposits produced in subsequent reforming experiments, as described in Section 2.2, were analysed by SEM. It was shown that they are also in the form of CNF, however, it was also observed that the subsequent CNF materials have narrower size distributions than the first generation CNF (Fig. 9b). The other difference lies in the quantity of encapsulated catalyst particles found in the CNF. SEM analyses show that the quantity of the catalyst particles, detected by SEM analysis, decreases over successive reforming experiments (Fig. 9b). As is seen in Table 2, this observation was confirmed by the quantity of Fe, obtained by means of AA analyses of successive generations of CNF. As expected due to the addition of the new CNF, it was found that the %w/w of Fe is reduced through each successive generation of the CNF.

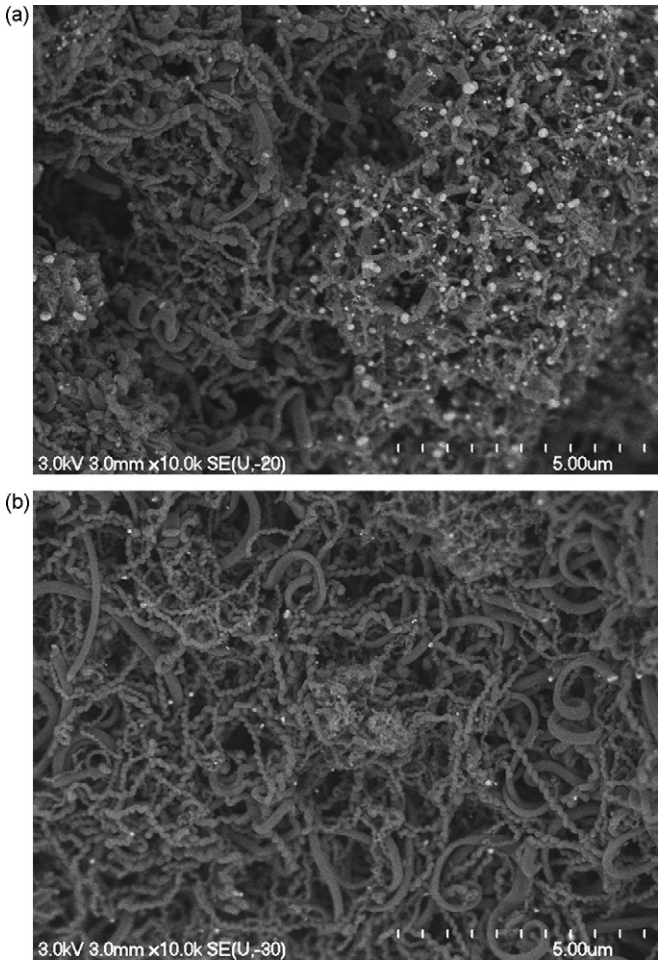

Fig. 9. (a) First-generation CNF. (b) Third-generations CNF.

XRD analyses were carried out on the CNF from different generations. Graphite and two types of iron carbides are shown to be the crystalline phases present in the CNF (Fig. 5). For the first generation, produced via the ethanol dry reforming process on the carbon steel catalyst, a sample of the thin layer of carbon, deposited directly on the surface of the steel, was analysed separately from the bulk of the carbon. As can be seen in Fig. 10, the carbon sample taken from the thin carbon layer, deposited directly on the carbon steel surface, contains higher concentrations of iron carbides, compared to samples taken from the bulk carbon nano-filaments (Fig. 5). This observation is in agreement with our microscopic observations of catalyst particles present in the thin layer of the first generation CNF, deposited directly on the surface of the carbon steel catalyst.

The XRD analyses show significant differences between the spectrum of the first generation CNF, and the spectrum of successive CNF generations (Fig. 11a and b). This difference is related to the heights and widths of the peaks associated with iron carbide and graphite. In the first generation CNF, the iron carbide peaks are very well defined. As we go forward through our successive experiments, these peaks become broader; perhaps an indication of the formation of new crystalline phases or products having smaller iron carbide particles [11]. It is also important to note that the height of the peak related to the presence of graphite ($2\theta = 26.3^\circ$), increases with the number of the CNF generation. It is observed in Fig. 11a, that the greatest concentration of iron carbide is that of the sample taken from the first generation CNF. However, it is also seen that no significant

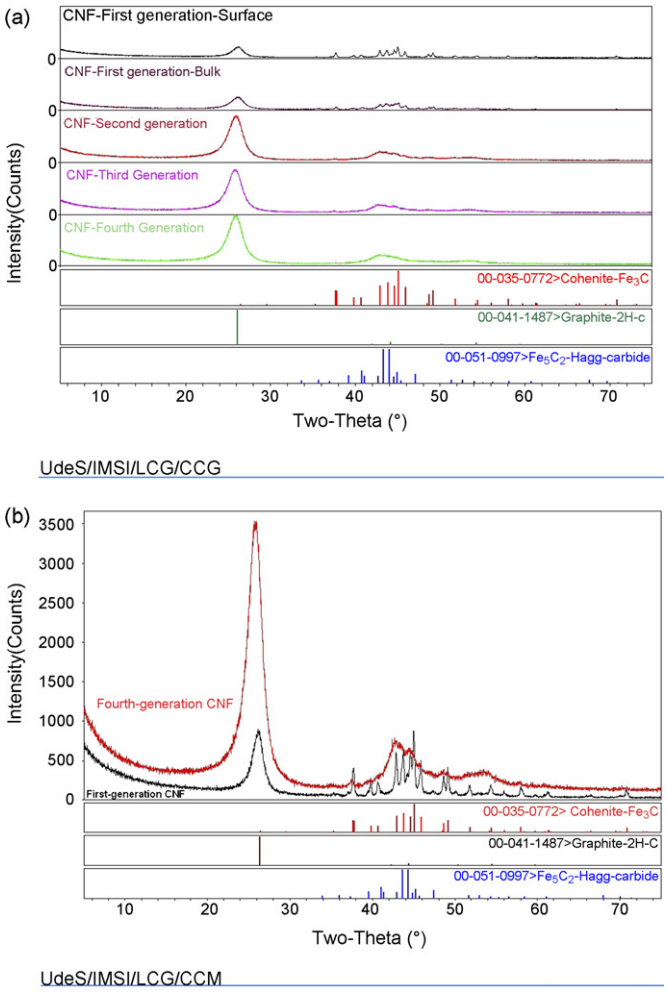

Fig. 11. (a) Comparison of XRD analyses of successive CNF generations. (b) Comparison of XRD analyses of first and the successive CNF generations.

difference is observed between successive generations, beyond the second generation.

4. Discussion

SEM analysis of the primary CNF shows several catalyst particles encapsulated within the nano-filaments (Fig. 9). Elemental analysis of these particles (Fig. 8) shows that they are composed of Fe and carbon. XRD analysis of the CNF (Fig. 11) detects two types of iron carbide in the produced CNF, in addition to the graphite phase. Based on the results of the above analyses, it is confirmed that the encapsulated particles, as found in the CNF by SEM analyses, are composed of iron carbide. It is therefore concluded that iron carbide particles, formed during the dry reforming of ethanol on the surface of the carbon steel, were then separated from the metal surface and encapsulated in the CNF.

The results of the series of reforming reactions, as summarised in Table 1, prove that first generation CNF have the greatest catalytic activity in the ethanol dry reforming reaction. As we progress over the series of successive experiments, using the CNF derived from the first generation to the fourth generation tests, the conversion of both ethanol and CO_2 decrease. This decrease is accompanied by decreasing volumes of produced H_2. This phenomenon can be explained by relating the catalytic properties of the CNF for promoting the ethanol dry reforming reaction, as well as for the catalytic cracking of the EtOH, to iron carbide particles encapsulated within the CNF. The particular catalytic activity of the iron carbides has been reported in the literature by Sacco et al. [12], Ruston et al. [13], Boehm [14], Li et al. [11] and also by Emmenegger et al. [15].

As it has been described above, the particles identified by the SEM analyses are composed of iron carbide. By subdividing the homogenised CNF product produced during each process step, each succeeding generation of the CNF product contains lesser amounts of iron carbide than its predecessor. Therefore, based on the amounts of iron present, determined by AA analyses, the third generation CNF has only 0.16 of the iron quantity present in the first generation CNF. Consequently, the values of GHSV, generated in the tests producing the second and fourth generation CNF, would be 121 000 ml/(min g) and 790 000 ml/(min g) respectively, based on the quantity of Fe involved (Table 2). By comparing the ethanol and CO_2 conversions, as well as the volume of hydrogen produced for these two experiments, it can be seen that the catalytic "activity" of third generation CNF is lower than that of first generation CNF. However, the change in the TOF values is nearly proportional to the quantities of iron present in the successive CNF generations; the very small deviations observed may be due to experimental errors and are not considered to be statistically significant. These results validate the iron carbide "hypothesis", i.e. their being the active catalysts involved in ethanol reforming. As seen in Table 1, following the third generation of CNF, the CO_2 conversion had fallen to zero, thus the series of "experiments" were stopped at the CNF fourth generation. However, it is also seen that, even when the conversion of CO_2 is reduced to zero, ethanol is still "converted" at the 90% level and the high hydrogen volumes are still produced. This is an indication that ethanol cracking is also catalysed by the CNF.

The "carbide" hypothesis is in general agreement with the "nano-filaments formation" general mechanism, proposed by Alstrup et al. [16], Teresa Tavares et al. [17], Kock et al. [18], Sacco et al. [12], Baker et al. [19], Rostrup-Nielsen and Trimm [20], Klop et al. [21], as well as with the reaction models reported by Alstrup [16], De Jong and Geus [22] and Ermakova et al. [23]. Ermakova et al. [23] reported the so-called carbide Fe_3C cycle suggested by Buyanov, for the mechanism of the growth of carbon filaments over iron based catalysts. On the basis of this model, as reported by Ermakova et al. [23] and De Jong and Geus [22] the hydrocarbon gas dissociates fully to separate carbon and hydrogen atoms, on the metal surface. The H_2 molecules then desorb, while the solid carbon dissolves in the bulk metal and forms metal carbides. The metal carbides then decompose to separate metal particles and molecular graphite. Individual metal particles are squeezed out because of the increasing internal pressure due to graphite layer formation at the internal surfaces of the graphite envelope and the liquid-like behaviour of the metal phase under these conditions. As soon as the free metal phase is forced out the fresh particle surface is exposed to the hydrocarbon and the growth continues.

The same mechanism can now also be reasonably proposed to explain the catalytic properties of the CNF. The preliminary CNF material encapsulates several iron carbide particles, most often at their "extended" tips. The reactants, ethanol and CO_2 in this case, are adsorbed, then decomposed and being involved in reactions on these particles' surfaces. Through the carbon phase deposited during this reaction, the growth of the CNF is able to continue at the rear surfaces of these iron carbide particles, or newly formed CNF may nucleate as well. However, the details of this nucleation mechanism are, as yet, unknown and additional work is required to elucidate the mechanism.

5. Conclusion

The results of this study confirm that CNF produced by the dry reforming of ethanol, using low-carbon steel as a catalyst, are active in the reactions of ethanol dry reforming and ethanol cracking, under the reaction conditions studied in this work. They are also able to sequester carbon in the form of CNF. The reactivity of the so-produced CNF, has proved to be related to iron carbide particles, encapsulated in their structures, and it is shown that the reactivity depends on the concentration of iron carbides present; i.e., the higher the concentration of iron carbides, the more active are the CNF particles. The mass of the CNF, used as the catalyst, was increased by 100% and 180% through the ethanol reforming and ethanol cracking reaction tests, respectively. Carbon deposits, generated during these reactions, were shown to be made of CNF particles, of a lower average diameter than the primary CNF. These deposits contain considerable amounts of CNF particles, with diameters falling within the range of 5–50 nm.

Acknowledgements

The authors are indebted to NSERC for the funding of this project. Special thanks are due to Mr. Peter Lanigan and Mr. Ovid Da Silva for reviewing the manuscript, to Mrs. Irène Kelsey for the SEM and XRD analyses and also to Mr. Henri Gauvin for his technical support.

References

[1] G. Xu, W. Wu, Y. Wang, W. Pang, Q. Zhu, P. Wang, Y. You, Constructing polymer brushes on multiwalled carbon nanotubes by in situ reversible addition fragmentation chain transfer polymerization, Polymer 47 (2006) 5909–5918.

[2] G.M. Kim, G.H. Michler, P. Pötschke, Deformation processes of ultrahigh porous multiwalled carbon nanotubes/polycarbonate composite fibers prepared by electrospinning, in: Proceeding of the 2nd BAF symposium, vol. 46, 2005, pp. 7346–7351.

[3] N. Meng, An overview of hydrogen storage technologies, Energy Explor. Exploit. 24 (2006) 197–209.

[4] Z. Sui, W. Yuan, Y. Dai, J. Zhou, Oxidative dehydrogenation of propane over catalysts based on carbon nanofibers, Catal. Today 106 (2003) 90–94.

[5] R.T.K. Baker, C.A. Bessel, K. Laubernds, N.M. Rodriguez, Graphite nanofibers as an electrode for fuel cell applications, J. Phys. Chem. B 105 (2001) 1115–1118.

[6] R.T.K. Baker, F. Salman, C. Park, Hydrogenation of crotonaldehyde over graphite nanofiber supported nickel, Catal. Today 53 (1999) 385–394.

[7] M.J. Ledoux, C. Pham-Huu, N. Keller, R. Vieira, New catalytic phenomena on nanostructured (fibers and tubes) catalysts, J. Catal. 216 (2003) 333–342.

[8] N. Abatzoglou, J. Blanchard, H. Oudghiri-Hassani, S. Jankhah, F. Gitzhofer, The DRIVE2 process for carbon sequestration through dry reforming of ethanol using iron catalysts, WSEAS Trans. Environ. Dev. 1 (2006) 15–21.

[9] N. Abatzoglou, J. Blanchard, H. Oudghiri-Hassani, S. Jankhah, F. Gitzhofer, The use of catalytic reforming reactions for CO_2 sequestration as carbon nanotubes, in: Proceedings of the 2006 IASME/WSEAS International conference on Energy and Environmental Systems, Chalkida, Greece, May 8–10, 2006, pp. 21–26.

[10] M. Boudart, Turnover rates in heterogenous catalysis, Chem. Rev. 95 (1995) 661–666.

[11] C. Li, Y. Fu, G. Bian, Y. Xie, T. Hu, J. Zhang, Effect of Seam in CO_2 reforming of CH_4 over a Ni/CeO_2–ZrO_2–Al_2O_3 catalyst, Kinet. Catal. 45 (2004) 679–683.

[12] A. Sacco, P. Thacker, T. Nan Chang, A.T.S. Chiang, The initiation and growth of filamentous carbon from a-iron in H_2, CH_4, H_2O, CO_2, and CO gas mixtures, J. Catal. 85 (1984) 224–236.

[13] W.R. Ruston, M. Warzee, J. Hennaut, J. Waty, The solid reaction products of the catalytic decomposition of carbon monoxide on iron at 550 °C, Carbon 7 (1969) 47–50.

[14] H.P. Boehm, Carbon from carbon monoxide disproportionation on nickel and iron catalysts: morphological studies and possible growth mechanisms, Carbon 11 (1973) 583–586.

[15] C. Emmenegger, J-. Bonard, P. Mauron, P. Sudan, A. Lepora, B. Grobety, A. Zuttel, L. Schlapbach, Synthesis of carbon nanotubes over Fe catalyst on aluminium and suggested growth mechanism, Carbon 41 (2003) 539–547.

[16] I. Alstrup, A new model explaining carbon filament growth on nickel, iron, and Ni–Cu alloy catalysts, J. Catal. 109 (2006) 241–251.

[17] M. Teresa Tavares, C.A. Bernardo, I. Alstrup, J.R. Rostrup-Nielsen, Reactivity of carbon deposited on nickel-copper alloy catalysts from the decomposition of methane, J. Catal. 100 (1986) 545–548.

[18] A.J.H.M. Kock, P.K. De Bokx, E. Boellaard, W. Klop, J.W. Geus, The formation of filamentous carbon on iron and nickel catalysts II Mechanism, J. Catal. 96 (1985) 468–480.

[19] R.T.K. Baker, P.S. Harris, R.B. Thomas, R.J. Waite, Formation of filamentous carbon from iron, cobalt and chromium catalyzed decomposition of acetylene, J. Catal. 30 (1973) 86–95.

[20] J. Rostrup-Nielsen, D.L. Trimm, Mechanisms of carbon formation on nickel-containing catalysts, J. Catal. 48 (1977) 155–165.

[21] W. Klop, J.W. Geus, E. Boellaard, P.K. de Bokx, A.J.H.M. I. Kock, Thermodynamics The formation of filamentous carbon on iron and nickel catalysts, J. Catal. 96 (1985) 454–467.

[22] P.K. De Jong, J.W. Geus, Carbon nanofibers: catalytic synthesis and application, Catal. Rev. Sci. Eng. 42 (4) (2000) 481–510.

[23] M.A. Ermakova, D.Y. Ermakov, A.L. Chuvilin, G.G. Kuvshinov, Decomposition of methane over iron catalysts at the range of moderate temperatures: the influence of structure of the catalytic systems and the reaction conditions on the yield of carbon and morphology of carbon filaments, J. Catal. 201 (2001) 183–197.